Chinese Chemical Letters 33 (2022) 4583–4586

Contents lists available at ScienceDirect

Chinese Chemical Letters

journal homepage: www.elsevier.com/locate/cclet

A glutathione activatable pro-drug-photosensitizer for combined chemotherapy and photodynamic therapy

Yanjun Yang[a], Yifeng Zhang[a], Ran Wang[a], Xiang Rong[a], Ting Liu[a], Xiang Xia[a], Jiangli Fan[a,b], Wen Sun[a,b,*], Xiaojun Peng[a]

[a] State Key Laboratory of Fine Chemicals, Dalian University of Technology, Dalian 116024, China
[b] Ningbo Institute of Dalian University of Technology, Ningbo 315016, China

ARTICLE INFO

Article history:
Received 27 December 2021
Revised 4 March 2022
Accepted 9 March 2022
Available online 13 March 2022

Keywords:
Pro-drug-photosensitizer
Chemotherapy
Photodynamic therapy
GSH activation

ABSTRACT

During cancer treatment, chemotherapeutic drugs always result in severe side-effects and drug resistance. Therefore, combining cheomtherapy with other therapeutic modalities, such as photodynamic therapy (PDT) and designing an activable platform is promising for precise and efficient anticancer treatment. Herein, we report a "pro-drug-photosensitizer" agent, LMB-S-CPT, bearing a disulfide bond as the glutathione (GSH)-activatable linker. LMB-S-CPT can be selectively activated by GSH to release activated drug, camptothecin (CPT), for chemotherapy and activated photosensitizer, methylene blue (MB), for PDT. LMB-S-CPT exhibits excellent tumor-activatable performance when injected into tumor-bearing mice, as well as specific cancer therapy with negligible toxic side effects. The activatable pro-drug-photosensitizer offers a new strategy for chemo-photodynamic therapy and displays precise, selective and excellent antitumor effect.

We presented a "pro-drug-photosensitizer" agent, LMB-S-CPT. LMB-S-CPT can be selectively activated by GSH to release activated drug, camptothecin (CPT), and activated photosensitizer, methylene blue (MB). It offers a new strategy for chemo-photodynamic therapy and displays excellent antitumor effect.

Chemotherapy is one of the most important approaches in cancer treatment, which is impeded by its severe side-effects to normal cells and tissues due to its nonselectivity and high toxicity [1–4]. In addition, cancer cells become drug resistant after several course of treatments, resulting in inefficient therapeutic [3]. To overcome the limitations of conventional chemotherapeutic drugs, various drug delivery systems (DDS) and tumor specific prodrugs have been explored [5–11]. Based on these platforms, the precise drug release is achieved by responding to tumor microenvironment (TME) such as glutathione (GSH), enzymes or reactive oxygen to distinguish tumor tissue from normal tissue [12–17]. Especially, the prodrugs, becoming nontoxic to highly toxic in tumor cells *via* specific activation can be further combined with fluorescent reporters, to enable fluorescence diagnosis of cancer and real-time monitoring the activation of prodrugs [8,9,18-22].

Previously reported prodrug strategies only involve single chemotherapy, which makes treatment limited owning to the tumor heterogeneity [1–4]. In recent years, the combination of multiple therapeutic modalities has attracted an increasingly attention [23]. Animal pre-clinical experimental data has shown that photodynamic therapy (PDT) can supplement with chemotherapy to achieve a cure for cancer [24–26]. During PDT, photosensitizer (PS) can sensitize oxygen into reactive oxygen species (ROS) under light irradiation, which, as highly oxidizing species can cause tumor cell apoptosis or necrosis [26,27]. The different mechanisms of chemotherapy and PDT can conquer the drawback of single treatment and enhance the therapeutic efficiency [28–31]. Current excising PSs are always "on" and non-specific to tumor cells, which could accumulate in normal tissues and may lead to side effects when exposed to light radiation [30,32]. Similar to prodrug strategy, pro-photosensitizers which are activated by tumor-selective species can also help to improve the selectivity to tumor cells and reduce the non-desired damages [25,33]. Among different PSs, methylene blue (MB) is the clinically used one with high singlet oxygen ($^1O_2$) quantum yield [34,35]. More importantly, MB can be reduced into its inactive stage, leucomethylene blue (LMB), demonstrating no absorbance and fluorescence. LMB can be easily oxidized to MB in the presence of oxygen and become active under light [36,37]. We thus speculate that LMB derivatives can be used to design a pro-photosensitizer, which can be further combined with prodrug for the combination of PDT and chemotherapy.

* Corresponding author.
E-mail address: sunwen@dlut.edu.cn (W. Sun).

https://doi.org/10.1016/j.cclet.2022.03.040
1001-8417/

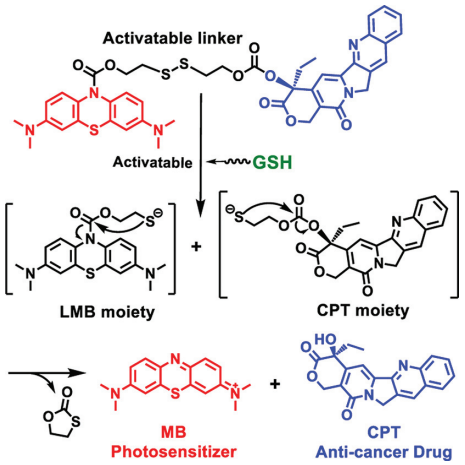

Fig. 1. The MB and CPT release mechanism of the activable LMB-S-CPT by GSH.

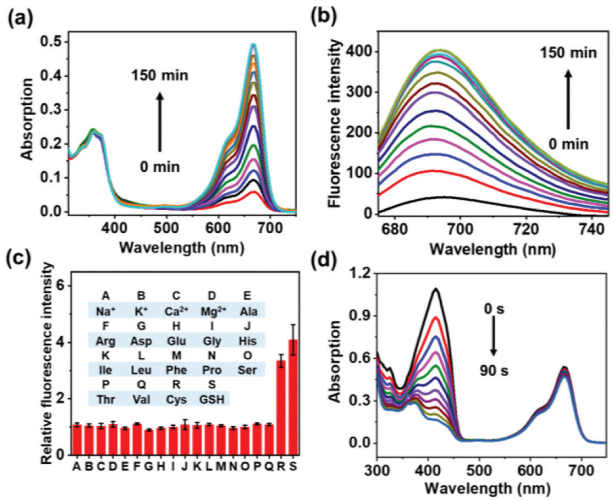

Fig. 2. The absorption (a) and emission (b) changes of LMB-S-CPT (10 μmol/L) in the presence of GSH (2.5 mmol/L, 250 equiv.) in DMSO/PBS solution (50/50, v/v) over time. (c) The relative fluorescence intensity charge of LMB-S-CPT under common amino acids and metal ions (2.5 mmol/L, 250 equiv.). (d) The absorbance decreases of DPBF at 415 nm with red light irradiation (660 nm, 1 mW/cm^2) in the present of activated LMB-S-CPT.

Herein, we report a novel GSH activatable "pro-drug-photosensitizer" (LMB-S-CPT) for the combination of PDT and chemotherapy with red light irradiation. LMB and camptothecin (CPT) are linked by disulfide bond to construct LMB-S-CPT. In health tissues or organs, non-cytotoxicity can be detected because the activity of both PS and drugs are inhibited in the presence of disulfide bonds. However, when the conjugate is uptaken by cancer cells, the disulfide bond is reduced by excessive GSH to release LMB and CPT. Subsequently, LMB is rapidly oxidized to MB which can generate $^1O_2$ upon the red-light irradiation for PDT. LMB-S-CPT as a novel "pro-drug-photosensitizer" design, for the first time achieves the combination of chemotherapy and PDT.

LMB-S-CPT was synthesized through a multi-step route as shown in Fig. S1 (Supporting information). MB was reduced by sodium dithionite to produce LMB, the reduced form of methylene blue, which further reacted with triphosgene to yield LMBCl. Similarly, CPT-S was synthesized from CPT that reacted with triphosgene and then 2,2′-dithiodiethanol. The final compound, LMB-S-CPT was obtained through the coupling of LMBCl and CPT-S in the present of sodium carbonate and 4-dimethylaminopyridine (DMAP). The final compound and important intermediates were characterized by nuclear magnetic resonance (NMR) and high-resolution mass spectrometry (HRMS) (Figs. S13 and S21 in Supporting information).

The disulfide bond of LMB-S-CPT could be cut off by biothiols, such as GSH, which is excessive in tumor cells. The reaction mechanism of LMB-S-CPT with GSH is shown in Fig. 1. The breakage of disulfide bond by reduced GSH triggered the intramolecular cyclization, resulting in the fluorescence recovery of MB and the release of CPT. Firstly, we studied the activable properties of LMB-S-CPT by GSH (Figs. 2a and b). LMB-S-CPT exhibited weak absorption and emission at 665 nm and 695 nm in DMSO/PBS solution (50/50, v/v), respectively (Fig. S2 in Supporting information). Upon the addition of GSH (250 equiv., 2.5 mmol/L), significant fluorescent enhancement was observed (Fig. 2b). We speculated that the large fluorescence recovery was attributed to GSH-induced cleavage of the disulfide bond, which released free MB. In addition, CPT was also release *via* the similar intramolecular cyclization. The reaction products were further verified by ESI-MS. Mass peaks at $m/z = 284.1212$ $[M]^+$ corresponding to MB and $m/z = 349.1176$ $[M+H]^+$ corresponding to CPT were simultaneously detected (Fig. S3 in Supporting information). The reaction kinetics of LMB-S-CPT with GSH was further investigated. The reaction initiated immediately once GSH was added to the solution of LMB-S-CPT, and fluorescence intensity reached a plateau within 150 min. The selectivity of LMB-S-CPT towards biothiols were investigated in the presence of others common amino acids and metal ions including Na^+, K^+, Ca^{2+}, Mg^{2+}, Ala, Arg, Asp, Glu, Gly, His, Ile, Leu, Phe, Pro, Ser, Thr, Val, Cys and GSH. The fluorescence of LMB-S-CPT demonstrated *ca.* 4-fold improvement at 695 nm in the response to biothiols like GSH and Cys (Fig. 2c). Conversely, almost no fluorescence enhancement was induced by other biologically analytes compared to the control group (Fig. 2c). Further, we measured the release efficiency of MB and CPT by the UV–visible absorption spectrum. The MB and CPT release efficiency of LMB-S-CPT exceeded 80% after incubation with GSH (Fig. S4a in Supporting information). The color of LMB-S-CPT solution became blue in the presence of GSH than that without GSH (Fig. S4b in Supporting information). In addition, LMB-S-CPT after activation by GSH showed almost the same absorption and fluorescence spectra compared with free MB at the same concentration, further indicating that MB was almost thoroughly released from LMB-S-CPT triggered by GSH (Figs. S4a and S5 in Supporting information).

It is well known that MB is a photosensitizer with excellent $^1O_2$ production quantum yield, but its reduced form cannot induce $^1O_2$ generation. A $^1O_2$ capture agent, 1,3-diphenlisobenzofuran (DPBF), was added to the solution of LMB-S-CPT and GSH-activated LMB-S-CPT, respectively. The absorption of DPBF at 415 nm was investigated to study the $^1O_2$ generation capacity. The absorbance of DPBF decreased significantly in LMB-S-CPT in the presence of GSH under 660 nm red light (1 mW/cm^2), which was almost the same as that of free MB (Fig. 2d, Fig. S6 in Supporting information). However, the absorption of DPBF and LMB-S-CPT mixed solution without GSH only caused slight decreased at 415 nm under the same conditions (Fig. S6). These results indicated that LMB-S-CPT was an activable PS whose PDT activity could be enhanced by intracellular GSH.

We evaluated the intracellular fluorescence recovery of LMB-S-CPT in both cancer (MCF-7 and 4T1) and normal cell lines. The fluorescence of LMB-S-CPT was significant elevated after incubation MCF-7 cells with the conjugate for 1 h. However, the negligible fluorescence increase was detected in 3T3 cells (Fig. S7 in Supporting information). Thus, MB could be released from LMB-S-CPT only in cancer cells due to the high level of GSH expression. Subsequently, the anticancer effect was studied. The cytotoxicity of LMB-S-CPT was investigated by 3-(4,5-dimethylthiazol-2-yl)−2,5-

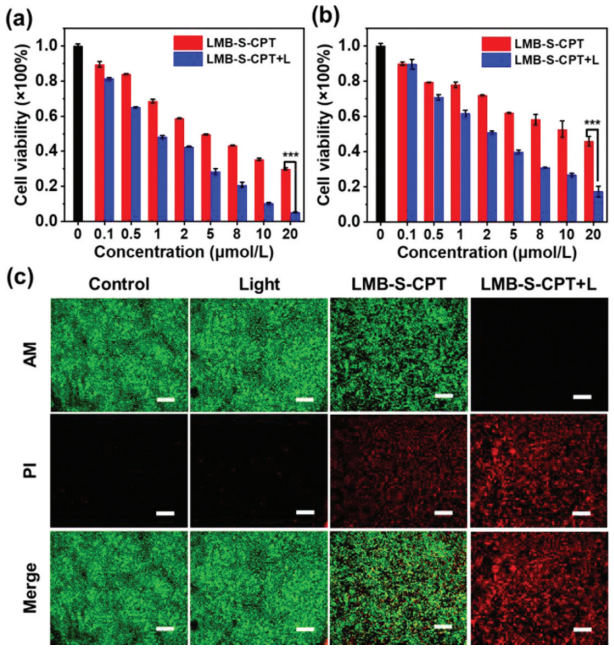

Fig. 3. Cytotoxicity of LMB-S-CPT in MCF-7 cells (a) and 4T1 cells (b) with or without red light irradiation (660 nm, 10 mW/cm^2, 10 min). (c) Confocal fluorescence images of live/dead cells. Scale bars: 400 μm. $^{***}P < 0.001$ determined by T-test.

diphenyl tetrazolium bromide (MTT) assay. MCF-7 cells, 4T1 cells and Hegp-2 cells were incubated with different concentrations of LMB-S-CPT. The cell viability was reduced to a certain extent with the treatment of LMB-S-CPT in the dark, which was attributed to the release of CPT due to the breakage of disulfide bonds by GSH (Figs. 3a and b, Fig. S8 in Supporting information). Once the red-light irradiation, a large percentage of tumor cells were killed by LMB-S-CPT (Figs. 3a and b). The cytotoxicity of LMB-S-CPT was significantly enhanced because the breakage of disulfide bonds realized the combined chemotherapy and PDT under red light irradiation. The cytotoxicity was further studied by calcein acetoxymethyl ester (calcein-AM) and propidium iodide (PI). Calcein-AM emitted green fluorescence in living cells, and PI emitted red fluorescence in dead cells. As shown in Fig. 3c, both green and red fluorescence with similar intensity was observed after incubation the cells with LMB-S-CPT, indicating that LMB-S-CPT exhibited sole chemotherapeutic effect in the dark. In addition, intensive red fluorescence emerged from the cells that were treated with LMB-S-CPT and red light (Fig. 3c). The results were similar to the trends in cell viability, which further illustrated that LMB-S-CPT realized the combination of chemotherapy and PDT under red light irradiation.

Subsequently, 2,7-dichlorofluorescein diacetate (DCFH-DA) was used to track the intracellular $^1O_2$ generation. DCFH-DA without fluorescence in living cells, can be hydrolyzed by intracellular esterase and further oxidized by ROS to generate 2,7-dichlorofluoresce (DCF), emitting obvious fluorescence. The cells showed almost no fluorescence when treated with LMB-S-CPT in the dark. Upon the red-light irradiation, strong fluorescence was observed in the cells that were pre-incubated with LMB-S-CPT (Fig. 4a). The results revealed that the GSH-responsive LMB-S-CPT could generate $^1O_2$ as an activable PS to achieve PDT. Next, annexin V-FITC (AV)/propidium iodide (PI) apoptosis detection kit was applied to reveal the stages of cells death after incubation with LMB-S-CPT with or without red light *via* flow cytometry. The cells with the lack of membrane integrity can be stained by annexin V-FITC, demonstrating that the cells were in the early stages of apoptotic. PI could only through the destroyed cell membrane, therefore, the cells of advanced apoptotic were selectively stained. When treated

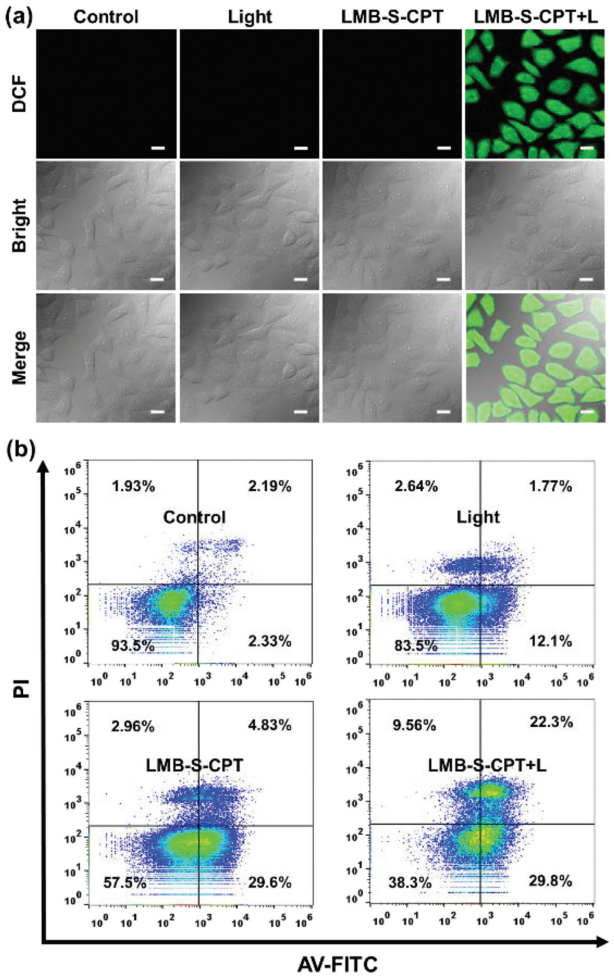

Fig. 4. (a) Intracellular ROS analysis by confocal fluorescence imaging in MCF-7 cells with different treatments (λ_{ex}: 488 nm and λ_{em}: 500–600 nm). Scale bars: 20 μm. (b) Flow cytometry analysis of apoptosis stage using AV-FITC and PI of MCF-7 cells with different treatments.

with LMB-S-CPT, the higher proportions of cells were in the early apoptosis stage compared to that of the control and light group (Fig. 4b). Upon red-light irradiation (660 nm, 10 mW/cm^2, 10 min), the amounts of cells in the late and early apoptotic stages significantly increased, indicating that the combination of chemotherapy and PDT demonstrated the superior effect of killing tumor cells compared to sole chemotherapy (Fig. 4b).

Given that LMB-S-CPT showed promising effect of PDT and chemotherapy *in vitro*, we evaluated the ability of anticancer effect in tumor-bearing mice. All animal experiments were performed in accordance with guidelines approved by the Ethics Committee of Dalian University of Technology (DUT20210902). 4T1 cells were injected subcutaneously into the armpits of the mice. When the tumor volume achieved to approximately 200 mm^3, the fluorescence recovery of LMB-S-CPT at the tumor site was determined. The fluorescence signal appeared at 0.5 h after injection, indicating that LMB-S-CPT was quickly activated by GSH and the MB and CPT were released in 4T1 tumor-bearing mice. In addition, the fluorescence intensity reached the peak at 2 h, which showed that this is the best time point for irradiation with red light (Fig. S9 in Supporting information). Therefore, 660-nm red light (50 mW/cm^2, 15 min) was used to irradiate tumors after 2 h injection of LMB-S-CPT. When investigated the anticancer effect, the 4T1 tumor-bearing mice were randomly divided into 4 groups: Mice were injected with PBS (control group); mice were only irradiated with

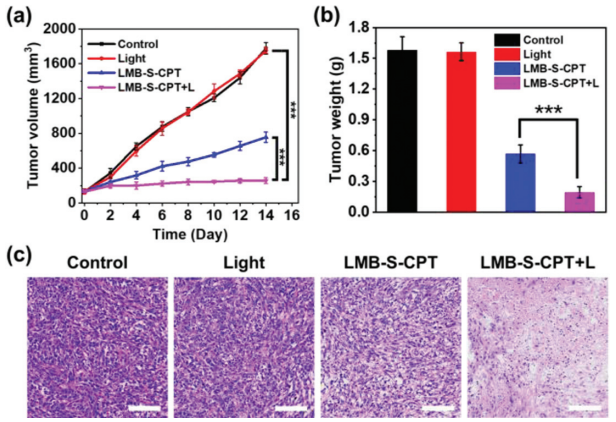

Fig. 5. The changes of (a) tumor volume and (b) tumor weight after different treatments. (c) Images of H&E staining of tumor tissue after different treatments. Scale bars: 100 μm. $^{***}P < 0.001$ determined by T-test.

660 nm red light after injection of PBS (light group); mice were intratumor injected with LMB-S-CPT (LMB-S-CPT group); mice were intratumor injected with LMB-S-CPT and irradiated with red light (660 nm, 50 mW/cm^2, 15 min) (LMB-S-CPT + L group). We recorded the tumor volume of the mice every other day. The mice in light group showed no appreciable differences in tumor growth compared to the control group. The injection of LMB-S-CPT inhibited the approximately 60% tumor growth because of sole CPT-mediated chemotherapy. The tumors were almost completely suppressed with the injection of LMB-S-CPT under the irradiation of red light, suggesting that the combination of PDT and chemotherapy demonstrated the most efficient anticancer effect (Fig. 5a). After the 14 days treatment, the mice were euthanized and the tumors were isolated. The weight of tumors and photographs of tumors further confirmed the tendency of tumors growth (Fig. 5b and Fig. S10 in Supporting information). The paraffin slices of tumors were made for hematoxylin and eosin (H&E) staining to evaluate the effect of tumor treatment. The tumors tissues were increasingly damaged in the LMB-S-CPT groups and LMB-S-CPT + L groups (Fig. 5c), suggesting that excellent therapeutic effect of LMB-S-CPT. LMB-S-CPT was superior *in vivo* physiological safety. The body weight of mice gradually grew amongst different groups, demonstrating that no additional side effects were observed during the whole experiment (Fig. S11 in Supporting information). The result also revealed the safety of light used in the experiment. The major organs including heart, liver, spleen, lung and kidney were dissected and the paraffin slices were made for hematoxylin and eosin (H&E) staining to evaluate biocompatibility. No significant pathological impairment occurred in the major organs (Fig. S12 in Supporting information), demonstrating that the systemic toxicity was not generated by LMB-S-CPT triggered chemo-photodynamic therapy under the activation of GSH and red-light irradiation.

In conclusion, we developed a novel GSH activatable pro-drug-photosensitizer, LMB-S-CPT, which was based on LMB and CPT linked by disulfide for combination of chemotherapy and PDT. The absorption and fluorescence of photosensitizer (MB) and toxicity of drug (CPT) were selectively activated by excessive GSH in tumor cells. Upon red light irradiation, LMB-S-CPT could produce cytotoxic $^1O_2$ for photodynamic therapy. Thus, LMB-S-CPT demonstrated the enhanced cytotoxicity and cell apoptosis compared to sole treatment. In addition, the anticancer effect of LMB-S-CPT was significantly elevated *in vivo* under red light irradiation. No apparent physiological toxicity was observed from major organs, suggesting the security and wonderful biocompatibility. LMB-S-CPT overcame the limitations of sole PDT or sole chemotherapy and provided a platform for activable pro-drug-photosensitizer with the enhanced antitumor effect.

Declaration of competing interest

The authors declare that they have no known competing financial interests or personal relationships that could have appeared to influence the work reported in this paper.

Acknowledgments

This work was supported by the National Natural Science Foundation of China (Nos. 22090011, 22078046, 21808028) and NSFC-Liaoning United Fund (No. U1908202).

Supplementary materials

Supplementary material associated with this article can be found, in the online version, at doi:10.1016/j.cclet.2022.03.040.

References

[1] V.T. DeVita Jr., E. Chu, Cancer Res. 68 (2008) 8643–8653.
[2] G.S. Karagiannis, J.S. Condeelis, M.H. Oktay, Clin. Exp. Metastasis 35 (2018) 269–284.
[3] K. Nurgali, R.T. Jagoe, R. Abalo, Front. Pharmacol. 9 (2018) 245.
[4] X. Wu, R. Wang, S. Qi, et al., Angew. Chem. Int. Ed. 60 (2021) 15418–15425.
[5] F. Wang, K. Wang, Q. Kong, et al., Coord. Chem. Rev. 429 (2021) 213636.
[6] D. Shao, M. Li, Z. Wang, et al., Adv. Mater. 30 (2018) 1801198.
[7] W. Cai, J. Wang, C. Chu, et al., Adv. Sci. 6 (2019) 1801526.
[8] X. Wu, X. Sun, Z. Guo, et al., J. Am. Chem. Soc. 136 (2014) 3579–3588.
[9] M. Xiao, W. Sun, J. Fan, et al., Adv. Funct. Mater. 28 (2018) 1805128.
[10] Q. Liu, H. Wang, G. Li, et al., Chin. Chem. Lett. 30 (2019) 485–488.
[11] L. Zhao, Y. Xing, R. Wang, F. Yu, F. Yu, ACS Appl. Bio Mater. 3 (2020) 86–106.
[12] X. Xue, Y. Zhao, L. Dai, et al., Adv. Mater. 26 (2014) 712–717.
[13] Y. Zhou, M. Maiti, A. Sharma, et al., J. Control. Release 288 (2018) 14–22.
[14] X. Li, J. Kim, J. Yoon, X. Chen, Adv. Mater. 29 (2017) 1606857.
[15] F. Gong, N. Yang, X. Wang, et al., Nano Today 32 (2020) 100851.
[16] B. Sun, C. Luo, X. Zhang, et al., Nat. Commun. 10 (2019) 3211.
[17] A. Podder, S. Koo, J. Lee, et al., Chem. Commun. 55 (2019) 537–540.
[18] M. Zhao, B. Li, H. Zhang, F. Zhang, Chem. Sci. 12 (2020) 3448–3459.
[19] F. Ding, Z. Chen, W.Y. Kim, et al., Chem. Sci. 10 (2019) 7023–7028.
[20] W. Sun, S. Guo, C. Hu, J. Fan, X. Peng, Chem. Rev. 116 (2016) 7768–7817.
[21] X. Chen, D. Lee, S. Yu, et al., Biomaterials 122 (2017) 130–140.
[22] S. Lu, X. Lei, H. Ren, et al., ACS Appl. Bio. Mater. 3 (2020) 3835–3845.
[23] X. Li, J.F. Lovell, J. Yoon, X. Chen, Nat. Rev. Clin. Oncol. 17 (2020) 657–674.
[24] S.S. Lucky, K.C. Soo, Y. Zhang, Chem. Rev. 115 (2015) 1990–2042.
[25] Y. Chen, X. Zhao, T. Xiong, et al., Sci. China Chem. 64 (2021) 808–816.
[26] V.N. Nguyen, Y. Yan, J. Zhao, J. Yoon, Acc. Chem. Res. 54 (2021) 207–220.
[27] C. Ji, Q. Gao, X. Dong, et al., Angew. Chem. Int. Ed. 57 (2018) 11384–11388.
[28] C.Y. Sun, Z. Cao, X.J. Zhang, et al., Theranostics 8 (2018) 2939–2953.
[29] E. Chang, J. Bu, L. Ding, et al., J. Nanobiotechnol. 19 (2021) 154.
[30] K.M. Ihsanullah, B.N. Kumar, Y. Zhao, et al., Biomaterials 245 (2020) 119982.
[31] B. Chu, Y. Qu, X. He, et al., Adv. Funct. Mater. 30 (2020) 2005918.
[32] X. Zhang, Y. Chen, H. He, et al., Angew. Chem. Int. Ed. 60 (2021) 26337–26341.
[33] R. Wang, X. Xia, Y. Yang, et al., Adv. Healthcare Mater. 11 (2022) 2102017.
[34] T.T. Yao, J. Wang, Y.F. Xue, et al., J. Mater. Chem. B 7 (2019) 5089–5095.
[35] K. Yang, J. Wen, S. Chao, et al., Chem. Commun. 54 (2018) 5911–5914.
[36] P. Wei, L. Liu, Y. Wen, et al., Angew. Chem. Int. Ed. 58 (2019) 4547–4551.
[37] P. Wei, W. Yuan, F. Xue, et al., Chem. Sci. 9 (2018) 495–501.